Bifurcation theory for three-dimensional flow in the wake of a circular cylinder

Dwight Barkley*

Mathematics Institute, University of Warwick, Coventry CV4 7AL, United Kingdom

Laurette S. Tuckerman[†]

LIMSI-CNRS, Boîte Postale 133, 91403 Orsay Cedex, France

Martin Golubitsky[‡]

Department of Mathematics, University of Houston, Houston, Texas 77204

(Received 20 September 1999)

A bifurcation scenario is presented for three-dimensional vortex shedding in the wake of a circular cylinder for Reynolds numbers up to 300. Amplitude equations are proposed to describe the nonlinear interaction between two three-dimensional modes of shedding with different spanwise wave numbers and different spatiotemporal symmetries. The amplitude equations explain many features of the transition scenario observed experimentally.

I. INTRODUCTION

In this paper we consider the three-dimensional flow patterns produced in the wake of a circular cylinder. This classical flow problem is characterized by a single parameter, the Reynolds number $\mathrm{Re} \equiv U_\infty d/\nu$, where U_∞ is the fluid velocity far from the cylinder, d is the cylinder diameter, and ν is the kinematic viscosity for the fluid; see Fig. 1. The cylinder is assumed to be sufficiently long that it can be taken to be effectively infinite. At low Reynolds numbers the flow is steady and at $\mathrm{Re} \simeq 47$ the flow becomes unsteady in a Hopf bifurcation [1–3]. The resulting oscillatory flow leads to the shedding of alternating sign vortices from the cylinder: the Bénard–von Kármán vortex street [4,5]. This flow is nominally two-dimensional [6–8], i.e., the shed vortices are parallel to the axis of the cylinder. What is of interest here is the subsequent three-dimensional transitions that take place up to Reynolds numbers of about 300.

Experiments by Williamson [9] first established important features of three-dimensional vortex shedding patterns. Numerical stability computations have provided further quantitative data by establishing precise stability limits for the two-dimensional flow [10]. Williamson [11,12] reviews the experimental and computational studies of three-dimensional vortex shedding from circular cylinders. The following transition scenario is now established for Reynolds numbers up to 300. At $\mathrm{Re} = 189$ the two-dimensional wake becomes linearly unstable to a three-dimensional flow with a spanwise wavelength of 4 cylinder diameters. This shedding mode is called mode A. Experimentally [9] and computationally [13] mode A instability has been shown to be subcritical with a small range of hysteresis (about 10 Reynolds numbers). Experimentally, mode A is found to exhibit dislocations and

complex temporal behavior [11,14]; however, this aspect of the dynamics will not be considered here.

Above $\mathrm{Re} \simeq 260$, the flow is found experimentally to be in a different state: mode B. This state is characterized by a sharp frequency spectrum and a spanwise wavelength of about one cylinder diameter (approximately one fourth the wavelength of mode A). The state also is of a different symmetry type (described below). Linear stability results show that the two-dimensional wake becomes linearly unstable to mode B shedding at $\mathrm{Re} = 259$. Furthermore, this bifurcation is supercritical [15], i.e., the branch of mode B solutions bifurcates in the direction of increasing Reynolds number and pure mode B states do not exist below this Reynolds number.

In experiments [9,11,14], and to some degree in direct numerical simulations [15], it is found that the transition from mode A to mode B is gradual with energy in the flow shifting continuously from mode A to mode B over a range of Reynolds numbers starting at Re between 210 and 220 and ending at about $\mathrm{Re} = 270$. The transition is not hysteretic, rather it is a reversible interpolation between the two three-dimensional shedding modes.

In this paper we shall explain, from a bifurcation-theoretic viewpoint, how the entire transition scenario from two-
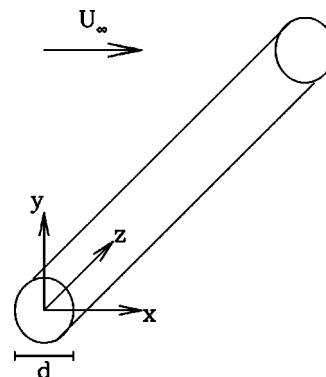

FIG. 1. Sketch of flow geometry.

---

*Electronic address: barkley@maths.warwick.ac.uk

†Electronic address: laurette@limsi.fr
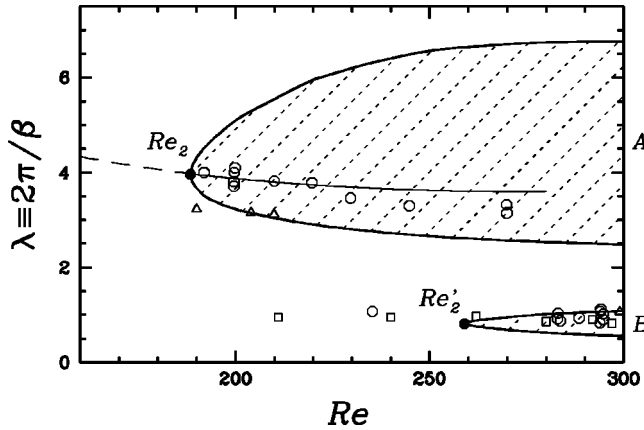
‡Electronic address: mg@math.uh.edu

FIG. 2. Regions (shaded) of linearly instability for the two-dimensional wake and the dominant spanwise wavelength observed in experiments (open symbols) from several groups Refs. [21–23]. The longer wavelength states correspond to mode A shedding and the shorter wavelength states to mode B shedding. This figure is reproduced with permission from Ref. [10].

dimensional shedding through various three-dimensional states is a natural consequence of interaction between the mode A and mode B instabilities of the two-dimensional wake. In particular we shall explain why it is possible to observe mode B well below linear instability threshold Re $=259$ and why there may be a gradual, non-hysteretic shift in energy between the two shedding modes over a range of Reynolds number.

II. PREVIOUS RESULTS

We begin by summarizing the numerical linear [10] and nonlinear [13,15] computations that will be used in the amplitude equations. While we shall make reference solely to these numerical results, because of their precision, they correspond quantitatively to experimental observations.

A. Linear results

The two-dimensional (2D) wake is a time-periodic flow of the form: $\mathbf{U}(x,y,t+T)=\mathbf{U}(x,y,t)$ where T is the vortex shedding period. The stability of $\mathbf{U}$ is characterized by the spectrum of Floquet multipliers μ for the linearized Navier-Stokes equations. The Floquet multipliers have been computed as a function of Reynolds number and spanwise wavelength λ. Figure 2 summarizes these results by showing the regions of the Re-λ parameter plane in which the 2D wake is linearly unstable, i.e., the regions for which there are Floquet multipliers outside the unit circle in the complex plane. In the unstable regions shown the multipliers are in fact real and positive with instability corresponding to $\mu>1$. The precise threshold values have been found for the two linear instabilities corresponding to mode A and mode B, respectively [10]: $\mathrm{Re}_c^A=189$, $\lambda_c^A=3.96$, and $\mathrm{Re}_c^B=259$, $\lambda_c^B=0.82$.

As noted by Williamson [12], mode A and mode B shedding have different symmetry types. This is apparent at the linear level as a difference in the spatio-temporal symmetries of the Floquet modes $\widetilde{\mathbf{u}}$ corresponding to the two bifurcations [10].

First note that 2D flow (base flow) has translational and reflectional symmetry in z:

$$\mathbf{U}(x,y,z,t)=\mathbf{U}(x,y,z+l,t), \tag{1}$$

$$\mathbf{U}(x,y,z,t)=\mathbf{U}(x,y,-z,t), \tag{2}$$

where l is an arbitrary real constant. These symmetries are trivial for the base flow because $\partial \mathbf{U}/\partial z=0$.

In addition, the 2D wake has the following spatio-temporal symmetry

$$U(x,y,z,t)=U(x,-y,z,t+T/2),$$

$$V(x,y,z,t)=-V(x,-y,z,t+T/2), \tag{3}$$

$$W(x,y,z,t)=W(x,-y,z,t+T/2).$$

That is, the flow is invariant under the combination of evolution by half a shedding period and reflection in y. We include the W component in Eqs. (3), even though $W=0$ for the base flow, because necessarily the three-dimensional flows (with $w\neq0$) that bifurcate will have symmetries that are a subset of symmetries (1)–(3).

The mode A instability breaks the translational symmetry along the cylinder so that the analog to symmetry (1) is satisfied for $l=n\lambda^A$ for all integers n. The instability does not break reflection symmetry (2) in z nor does it break spatio-temporal symmetry (3). Thus, the spatio-temporal symmetry of the Floquet mode A is [10]:

$$\widetilde{u}(x,y,z,t)=\widetilde{u}(x,-y,z,t+T/2),$$

$$\widetilde{v}(x,y,z,t)=-\widetilde{v}(x,-y,z,t+T/2), \tag{4}$$

$$\widetilde{w}(x,y,z,t)=\widetilde{w}(x,-y,z,t+T/2).$$

The mode B instability also breaks the translational symmetry so that the analog of Eq. (1) is satisfied for $l=n\lambda^B$ for all integers n. As with mode A, mode B does not break reflection symmetry (2) in z. However, it does break spatio-temporal symmetry (3). The spatio-temporal symmetry of the mode B Floquet mode is [10]:

$$\widetilde{u}(x,y,z,t)=\widetilde{u}(x,-y,z+\lambda^B/2,t+T/2),$$

$$\widetilde{v}(x,y,z,t)=-\widetilde{v}(x,-y,z+\lambda^B/2,t+T/2), \tag{5}$$

$$\widetilde{w}(x,y,z,t)=\widetilde{w}(x,-y,z+\lambda^B/2,t+T/2).$$

That is, mode B is invariant under the combination of evolution by half a shedding period, reflection in y, and translation in z by $\lambda^B/2$.

There are two further points concerning the linear analysis. The first is that all Floquet multipliers corresponding to 3D modes are double. This is a direct consequence of translational symmetry breaking. Specifically, the Floquet modes have trigonometric z-dependence and hence come in orthogonal pairs related by z translation (e.g., sine and cosine). The final point is that the linear terms in our amplitude equations will explicitly contain the Floquet multipliers, μ^A and μ^B, for the mode A and mode B instabilities. To obtain so-

lution branches with Reynolds number as the bifurcation parameter, we approximate the dependence of the multipliers on Reynolds number by linear functions. We have obtained from numerical computations

$$\mu^A(\text{Re}) = 1 + 0.0091(\text{Re} - 189) \qquad (6)$$

$$\mu^B(\text{Re}) = 1 + 0.021(\text{Re} - 259). \qquad (7)$$

B. Nonlinear results

The leading nonlinear classification of the mode A and mode B instabilities is as follows. Consider the dynamics of the stroboscopic or Poincaré map generated by the periodic flow. For mode A (mode B follows analogously) define A_n to be the complex amplitude whose magnitude corresponds to the magnitude of mode A shedding at the nth shedding cycle starting from some arbitrarily chosen reference time. Specifically, in numerical computations [13,15] the magnitude of A_n has been defined to be:

$$|A_n| \equiv \left[\frac{4}{\pi d^2 U_\infty^2} \int_\Omega |\hat{\mathbf{u}}^A|^2 d\Omega \right]^{1/2}, \qquad (8)$$

where Ω is the two-dimensional cross section of the computational domain and $\hat{\mathbf{u}}^A(x,y,t_n)$ is the coefficient of the Fourier transformation (in the spanwise direction) of the velocity field at the mode A wave number. The phase of A_n corresponds to the phase of mode A shedding along the cylinder and can be set to the phase of $\hat{\mathbf{u}}^A(x,y,t_n)$; however, the phase plays no significant role in the dynamics until quite high nonlinear order (see below).

Because the 3D Floquet multipliers are double, the mode A instability is a circle pitchfork bifurcation (pitchfork of revolution) for the map. To lowest nonlinear order the normal form governing the mode A bifurcation is

$$A_{n+1} = \mu^A A_n + \alpha_1^A |A_n|^2 A_n, \qquad (9)$$

where μ^A is the Floquet multiplier, Eq. (6), previously determined from the linear stability computations, and α_1^A is the Landau coefficient: if $\alpha_1^A < 0$, the instability is supercritical, else it is subcritical.

Making an analogous definition of B_n, a similar equation describes the mode B instability:

$$B_{n+1} = \mu^B B_n + \alpha_1^B |B_n|^2 B_n. \qquad (10)$$

Because μ^A and μ^B are known from the linear stability computations, it has been possible to determine the Landau coefficients α_1^A and α_1^B in Eqs. (9)–(10) from direct three-dimensional simulations starting near the linear instability thresholds [13,15]. The result is that $\alpha_1^A = 0.116 > 0$ and $\alpha_1^B = -3.92 < 0$, so that the mode A instability is subcritical and the mode B instability is supercritical.

III. AMPLITUDE EQUATIONS

We now consider a set of bifurcation equations describing the interaction of the mode A and mode B instabilities: the A-B mode interaction problem. Equations (9)–(10) describe

the dynamics up to third order in the absence of interaction. The task is to extend these to include the possibility of coupling between the A and B modes.

A. General

To obtain coupling terms we assume that somewhere in an extended parameter space there exists a point where the mode A and mode B instabilities occur simultaneously and that what is observed as a function of the single parameter, Reynolds number, is a path in the unfolding of this codimension-two point. This assumption, together with the wavelength ratio of the A and B modes and their symmetries, is sufficient to obtain the general form of the bifurcation equations.

While the derivation is in principle a straightforward application of methods of bifurcations with symmetry [16], taking into account all the details is quite involved, particularly because the bifurcations involve periodic orbits [17,18]. Here we justify the amplitude equations by outlining the procedure by which they could in principle be obtained with full rigor.

To handle the bifurcations from a periodic orbit in the presence of symmetry, one uses multiple Poincaré sections as in Refs. [17] and [18]. The result is a map capturing both the spatial and spatio-temporal symmetries of the problem. In our case the spatial symmetry corresponding to z translations and reflections, Eqs. (1)–(2), is given by the group $O(2)$. Spatio-temporal symmetry (3) becomes an additional reflection symmetry Z_2 for the map [18]. Because the spatio-temporal symmetry is a reflection, all bifurcations from the 2D branch necessarily either break the spatio-temporal symmetry of the 2D flow, as in mode B, or maintain the spatio-temporal symmetry, as in mode A. The full symmetry group for the problem is $\Gamma = O(2) \times Z_2$.

For A and B modes undergoing simultaneous instabilities there will be a four-dimensional center eigenspace with coordinates (A,B) in C^2. The symmetry-group elements can be taken to act on these coordinates as:

$$\theta(A,B) = (e^{i\theta}A, e^{im\theta}B),$$

$$\kappa_z(A,B) = (\bar{A}, \bar{B}),$$

$$\kappa(A,B) = (A, -B),$$

where θ is translation in z by $l = \theta \lambda^A/2\pi$, κ_z is z reflection with bar denoting complex conjugation, and κ represents the spatio-temporal symmetry (B breaks symmetry κ while A does not). We define $m \equiv \lambda^A/\lambda^B$ and assume for simplicity in this derivation that m is an integer. As we explain momentarily, this assumption is not essential.

The theory of bifurcations with symmetry [16] can now be used to derive the most general equations consistent with these symmetries. One finds a minimal set of three invariants

$$a \equiv |A|^2, \quad b \equiv |B|^2, \quad c \equiv (A^m \bar{B} + \bar{A}^m B)^2, \qquad (11)$$

and of four equivariants

$$(A, 0), \quad (\bar{A}^{2m-1} B^2, 0), \quad (0, B), \quad (0, A^{2m} \bar{B}). \qquad (12)$$

From this, the most general set of evolution equations is:

$$A_{n+1}=p(a,b,c)A_n+q(a,b,c)\bar{A}_n^{2m-1}B_n^2, \qquad (13)$$

$$B_{n+1}=r(a,b,c)B_n+s(a,b,c)A_n^{2m}\bar{B}_n, \qquad (14)$$

where p, q, r, and s are arbitrary real polynomial functions. These equations have been previously derived and partially investigated [19] in the context of the Faraday instability of a vertically vibrated fluid layer.

In deriving Eqs. (13)–(14) we have assumed $m=\lambda^A/\lambda^B$ to be an integer. Recall that the wavelength ratio of the two modes at their respective onsets is $\lambda_c^A/\lambda_c^B=3.96/0.82=4.83 \approx 5$. When the wavelengths of the two fastest growing modes are calculated at the same Reynolds number, the ratio between them varies between 4 and 5, depending on Reynolds number. Whether $m=4$ or $m=5$ is irrelevant to our considerations because the most important features of the A-B mode interaction are contained in low-order truncations of Eqs. (13)–(14). In particular, m does not appear in any fifth-order truncation as long as $m>2$, and for $m=4$ or $m=5$ the terms involving m are already of order nine or greater. If the wavelength ratio is taken to be a rational number between four and five, the terms depending on the wavelength ratio in the resulting equations will be of higher order still. In short, the ratio of mode A and mode B wavelengths does not enter the equations at low order and so is not relevant.

The phases of A and B only enter the dynamics nontrivially through the terms involving m and hence the truncations we consider leave the phases of A and B fixed. Note finally that the frequencies of the A and B modes do not appear in Eqs. (13)–(14) because these describe the dynamics of the Poincaré map. In an extended parameter space in which the instabilities occur simultaneously, the frequencies of the A and B modes would be equal at onset, each being equal to the frequency of the 2D wake at that point. The frequencies of these two three-dimensional modes will vary along solution branches as one moves away from the codimension two point. Hence, as observed in experiment, the mode A and mode B frequencies will not be equal in general, but can be expected to be comparable. This has no implications for our analysis.

B. Third order

Truncating Eqs. (13)–(14) at third order gives:

$$A_{n+1}=\mu^A A_n+\alpha_1^A|A_n|^2A_n+\gamma_1^A|B_n|^2A_n, \qquad (15)$$

$$B_{n+1}=\mu^B B_n+\alpha_1^B|B_n|^2B_n+\gamma_1^B|A_n|^2B_n. \qquad (16)$$

Thus at third order, two coupling terms appear. Consider first the effect of mode A on the mode B instability. Linearizing Eq. (16) about $B_n=0$ gives the linear stability equation for mode B:

$$B_{n+1}=(\mu^B+\gamma_1^B|A_n|^2)B_n. \qquad (17)$$

In the absence of mode A (i.e., $A_n=0$, corresponding to the basic 2D flow), the linear stability to B modes is determined simply from the Floquet multiplier μ^B, with instability oc-

curring in practice as μ^B crosses the unit circle at $+1$. In the presence of mode A there is a shift in the stability threshold by the amount $\gamma_1^B|A_n|^2$. If $\gamma_1^B>0$ then mode A has a destabilizing effect on mode B. This is the situation suggested by the experimental data in Fig. 2. A similar argument applies to the effect of mode B on mode A except that in this case the data suggest $\gamma_1^A<0$ since mode A shedding is suppressed as the Reynolds number is increased beyond the mode B instability threshold.

In principle one could numerically compute the coupling coefficients γ_1^A and γ_1^B using a method similar to that used to find the Landau coefficients α_1^A and α_1^B; however, this would first require a linear stability analysis of the fully three-dimensional mode A and mode B flow and this is a considerable undertaking. It is therefore necessary to estimate these coefficients based on the Reynolds number range of experimentally observed mode A and mode B states. In fact, these two coefficients can be determined uniquely given the Reynolds number at which mode B is first observed and the Reynolds number at which mode A is last observed. These criteria lead to $\gamma_1^A\simeq-22$ and $\gamma_1^B\simeq0.13$.

C. Fifth order

As was noted in Secs. I and II B, the mode A instability is subcritical with a small range of hysteresis in the transition from 2D shedding to mode A shedding. The amplitude equations at third order are not sufficient for describing this hysteresis. Thus, we must consider Eqs. (13)–(14) at next nonzero order:

$$A_{n+1}=\mu^A A_n+\alpha_1^A|A_n|^2A_n+\gamma_1^A|B_n|^2A_n+\alpha_2^A|A_n|^4A_n$$
$$+\gamma_2^A|B_n|^2|A_n|^2A_n+\gamma_3^A|B_n|^4A_n,$$

$$B_{n+1}=\mu^B B_n+\alpha_1^B|B_n|^2B_n+\gamma_1^B|A_n|^2B_n+\alpha_2^B|B_n|^4B_n$$
$$+\gamma_2^B|A_n|^2|B_n|^2B_n+\gamma_3^B|A_n|^4B_n.$$

Of the six fifth-order terms, only the term $\alpha_2^A|A_n|^4A_n$ has any effect on the pure A solution branch. With $\alpha_2^A<0$ this term will produce hysteresis in the mode A transition and α_2^A can be estimated from the range of hysteresis in simulations or experiment. The value $\alpha_2^A=-0.04$ gives a hysteresis of about 10 Reynolds numbers, consistent with observations.

While it is possible to conclude certain facts about the coefficients of the remaining fifth-order terms, (e.g., $\alpha_2^B\leqslant0$ else the pure B branch would have a saddle-node), the coefficients cannot be determined from current numerical and experimental data. Here we seek the minimal model necessary to account for the wake dynamics and therefore simply set these coefficients to zero. This gives the following system of equations describing the AB-mode dynamics of the cylinder wake:

$$A_{n+1}=\mu^A(\text{Re})A_n+\alpha_1^A|A_n|^2A_n+\gamma_1^A|B_n|^2A_n+\alpha_2^A|A_n|^4A_n,$$

$$B_{n+1}=\mu^B(\text{Re})B_n+\alpha_1^B|B_n|^2B_n+\gamma_1^B|A_n|^2B_n.$$

Figure 3 shows a bifurcation diagram for these equations. The Floquet multipliers depend on Reynolds number as given in Eqs. (6) and (7). The Landau coefficients have the
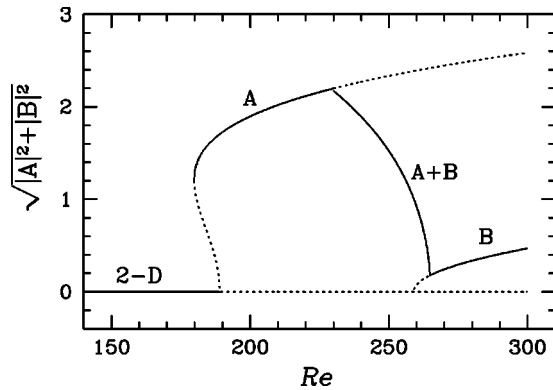
FIG. 3. Bifurcation diagram for amplitude equations. Shown are the steady states for these equations with solid lines indicating stable states. The 2D branch has $A = B = 0$. The A branch has $B = 0$, the B branch has $A = 0$, and the $A + B$ branch is a mixed-mode branch with both $A, B \neq 0$. The norm is $\sqrt{|A|^2 + |B|^2}$.

values $\alpha_1^A = 0.116$ and $\alpha_1^B = -3.92$ determined from nonlinear stability analysis as given in Sec. II B. We have set $\gamma_1^A = -22$, $\gamma_1^B = 0.13$, and $\alpha_2^A = -0.04$, as explained above, but the precise values of these three parameters are not important and the values should be taken to be representative.

The following scenario is found as a function of Reynolds number. The primary instability is to a pure mode A state at Re$= 189$. The instability is hysteretic with the mode-A branch extending down to Re$\simeq 180$. This upper branch is stable for a range in Reynolds number but becomes unstable at Re$\simeq 230$ to a branch of mixed-mode states in which both $A_n, B_n \neq 0$. This corresponds to the observation of both mode A and mode B wavelengths in experiment. The pure mode B branch bifurcates supercritically at Re$= 259$. This branch is initially unstable. The mixed-mode branch terminates on this pure mode B branch at Re$\simeq 265$ and above this Reynolds number only the pure mode B branch is stable. This corresponds to the experimental observation of only mode B wavelengths beyond this Reynolds number.

IV. CONCLUSIONS

A minimal system of amplitude equations has been proposed to account quantitatively for transitions between three-dimensional shedding modes in the wake of a circular cylinder. The equations explain both the experimental detection of mode B wavelengths below the mode B bifurcation point at Re$= 259$, and the nonhysteretic transition from mode A to mode B. These are all natural consequences of A-B mode interaction in which mode A has a destabilizing effect on mode B and mode B has a stabilizing effect on mode A with a resulting mixed-mode state over a range of Reynolds number.

The essential ingredients of the equations are the symmetries of the mode A and mode B states and how these dictate couplings between the two modes. There are relatively few terms in the equations at low orders and these have intuitive meanings, either as standard terms describing subcritical and supercritical bifurcations, or as couplings between modes with different symmetries. Many of the parameters are known from prior numerical computations and we have been able to estimate the coupling coefficients based on experimental data. In this work we have considered only the dynamics dictated by low-order truncations of the amplitude equations because these describe the most important bifurcations arising from the mode interaction. There will be effects, possibly including complicated spatio-temporal dynamics [19], due to the higher-order terms which we have ignored. However, near bifurcation, these effects are limited to narrow regions in parameter space.

We have not addressed here the important issue of dislocations and complicated temporal dynamics (broad-band frequency spectra) observed experimentally, particularly for mode A [11,14]. Leweke and Provansal have considered these dynamics within the framework of the complex Ginzburg-Landau (CGL) equation [20]. From this work it seems likely that the dislocations and complicated temporal dynamics observed in the cylinder wake are closely related to the spatio-temporal chaos found in this equation. However, the bifurcation structure of the CGL equation does not match what is known for the cylinder wake: in the CGL equation the instability of the periodic state (corresponding to instability of the 2D wake) is via the Benjamin-Feir instability with zero (spanwise) wavenumber, whereas for the cylinder wake there are two distinct linear instabilities of the 2D wake, each at finite wavenumber, giving rise to A and B branches. It would be of considerable interest to derive a model equation similar in spirit to the CGL equation considered by Leweke and Provansal, but which additionally contains naturally the symmetric bifurcation structure we have considered here.

[1] C. P. Jackson, J. Fluid Mech. **182**, 23 (1987).

[2] C. Mathis, M. Provansal, and L. Boyer, J. Fluid Mech. **182**, 1 (1987).

[3] J. Dusek, P. LeGal, and P. Fraunie, J. Fluid Mech. **264**, 59 (1994).

[4] H. Bénard, C. R. Acad. Sci. **147**, 839 (1908).

[5] T. von Kármán, Gottingen Nachr. Math. Phys. Kl. **12**, 509 (1912).

[6] C. H. K. Williamson, J. Fluid Mech. **206**, 579 (1989).

[7] M. Hammache and M. Gharib, Phys. Fluids A **1**, 1611 (1989).

[8] M. Hammache and M. Gharib, J. Fluid Mech. **232**, 567 (1991).

[9] C. H. K. Williamson, Phys. Fluids **31**, 3165 (1988).

[10] D. Barkley and R. D. Henderson, J. Fluid Mech. **322**, 215 (1996).

[11] C. H. K. Williamson, Annu. Rev. Fluid Mech. **28**, 477 (1996).

[12] C. H. K. Williamson, J. Fluid Mech. **328**, 345 (1996).

[13] R. D. Henderson and D. Barkley, Phys. Fluids **8**, 1683 (1996).

[14] C. H. K. Williamson, J. Fluid Mech. **243**, 393 (1992).

[15] R. D. Henderson, J. Fluid Mech. **352**, 65 (1997).

[16] M. Golubitsky, I. Stewart, and D. G. Schaeffer, *Singularities and Groups in Bifurcation Theory* (Springer, New York, 1988), Vol. II.

[17] B. Fiedler, *Global Bifurcation of Periodic Solutions with Symmetry*, Vol. 1309 of *Lecture Notes in Math.* (Springer, Berlin, 1988).

[18] J. S. W. Lamb and I. Melbourne, Arch. Ration. Mech. Anal. **149**, 229 (1999).

[19] J. Crawford, E. Knobloch, and H. Riecke, Physica D **44**, 340 (1990).

[20] T. Leweke and M. Provansal, Phys. Rev. Lett. **72**, 3174 (1994).

[21] C. H. K. Williamson, Phys. Fluids **8**, 1680 (1996).

[22] J. Wu, J. Sheridan, J. Soria, and M. C. Welsh, J. Fluid Struct. **8**, 621 (1994).

[23] H. Mansy, P.-M. Yang, and D. R. Williams, J. Fluid Mech. **270**, 277 (1994).